THE INFLUENCE ON THE PLASTIC WAVE PROPAGATION OF THE VARIATION OF YOUNG'S MODULUS WITH PLASTIC STRAIN

N. CRISTESCU,
University of Bucharest, Bucharest, Roumania
and
University of Florida, Gainesville, Florida, U.S.A.

ABSTRACT

The influence of the variation of Young's modulus with the plastic strain on the overall picture of the propagation of plastic waves in a bar, particularly on the unloading process, is examined here. The decrease of Young's modulus produces a decrease in velocity of propagation of the elastic unloading waves. Therefore, this velocity becomes variable from point to point in the bar, and the unloading process is generally delayed.

The results obtained by numerical integration of the equations of motion are compared with experimental data of J. F. Bell and with the computed case obtained by assuming E = constant.

1. INTRODUCTION

Although many experiments have shown that apparent elastic "constants" decrease during plastic deformation, the possible effects on the propagation of elastic unloading waves in dynamic problems have not been considered before. In this paper a law in which E varies with plastic strain is assumed, approximating the experimental results of Jukov [1].

In Jukov's experiments, tubular steel specimens were pulled in tension up to a certain plastic strain and then unloaded. A second loading, also in tension, followed the first one. During both unloading and reloading, Young's modulus was measured and compared with its initial value. By increasing, step by step, the maximum value of the plastic strain obtained in the first stage of the experiment, the variation of Young's modulus with respect to the plastic strain was obtained. Jukov has found that Young's mo-

dulus E always decreases with ε_p. For $\varepsilon_p = 2\ \%$, E decreases about 20 %. Similar results were obtained for the shear modulus, G.

It is very important to observe that the decrease of E with respect to ε_p is a time effect, since by remeasuring E in the tested specimens for extended intervals of time after the end of the first stage of the experiment, Jukov has found that E recovers in time and that after 80 days it had completely recovered its initial value. Taking into account that even between the unloading and reloading stages of the initial experiment, a time lapse of about a half an hour occurs, it is to be expected that in dynamic experiments when unloading follows loading after a very short interval of time, there is no time for E to recover, and thus the decrease of E with ε_p may possibly be much more significant than in static experiments. Other experiments in combined stresses performed by Jukov have shown that both elastic "constants" always decrease with any kind of plastic deformation.

The purpose of this paper is to study theoretically, within the classical framework of dynamic plasticity (i.e. stress-strain relation written in finite form, perfect elasticity during unloading, etc.), the influence of variation of E with ε_p during a dynamic unloading which follows a loading produced by plastic waves. Since the dynamic loading produces a nonhomogeneous distribution of plastic strains in the body, E will vary with position in the body. Thus, after a plastic deformation, an elastic unloading wave will propagate in the body with a speed variable from point to point.

To make the analysis more specific, a problem for which many experimental and analytical results are available in the literature will be considered. This is the classic one-dimensional problem of longitudinal plastic waves propagating in a bar. The bar will be assumed finite. At one end, an impact is produced while the other end is free. Thus the unloading will be initiated from this free end. Because a great amount of experimental data is available for symmetric longitudinal impact of two identical metallic bars, that problem is analyzed here. Thus the computed results, assuming E variable with ε_p, can be compared with the experimental results,

as well as with the computations performed under the assumption that E is constant during the whole loading-unloading process. A non-symmetric case can be analyzed by the same methods, althogh the symmetry assumption does save computation time, since the computations are carried out in one of the two bars only.

It is important to observe that the analysis presented here can be applied to any one-dimensional elastic-plastic dynamic problem concerning finite bodies as long as a single spatial coordinate is involved in the problem. In this paper we describe mainly the elastic non-homogeneity due to a plastic deformation. We may use the same procedure if the elastic unloading waves are propagating in a non-homogeneous heated body (either due to the plastic deformation itself or to other causes), or in a body subjected to repeated impacts where non-homogeneity due to plastic deformation can be more significant.

2. EQUATIONS OF THE PROBLEM

As is well known (see, for instance, Cristescu [2] Ch.II), in order to study the propagation of longitudinal elastic-plastic waves in thin bars of finite length, a quasilinear hyperbolic system of equations has to be solved

$$\frac{\partial v}{\partial t} = c^2(\varepsilon)\frac{\partial \varepsilon}{\partial x} \qquad (1)$$

$$\frac{\partial v}{\partial x} = \frac{\partial \varepsilon}{\partial t}$$

in the strip

$$0 < x < \ell \quad , \quad t > 0 \; . \qquad (2)$$

Here v is the particle velocity, $\varepsilon = \frac{\partial u}{\partial x}$ is a finite deformation measure; u, the displacement; x, the material coordinate; ℓ, the initial length of the bar; and $c(\varepsilon)$ is the variable velocity of the propagation of the waves.

Along the segment $0 < x < \ell$, $t = 0$ one has prescribed the "initial data" while along the lines $x = 0$, $t > 0$ and $x = \ell$, $t > 0$ the "boundary conditions" should be prescribed. For elastic-plastic materials in the strip (2) there will be two kinds of regions. In the "plastic" or "loading" region $c(\varepsilon) = \sqrt{\frac{1}{\rho}\frac{d\sigma}{d\varepsilon}}$ is to be calculated from the stress-strain law $\sigma = f(\varepsilon)$ accepted for the material considered, while in the "elastic" or

"unloading" region $c(\varepsilon_p(x))$ is constant in each section of the bar, but varies from section to section.

Therefore, in strip (2) two kinds of hyperbolic systems of the form (1) have to be solved; one is quasilinear (in the loading region) and the other semilinear (in the unloading region). Both regions are located in the strip (2), but the boundary between them is not known before solving the problem. For general boundary and initial conditions the problem is incompatible, unless the boundary between the two previously mentioned regions is found in an appropriate manner.

In order to give examples which would allow comparison of the results with the already computed cases where Young's modulus was assumed to be constant, the same stress-strain relation in finite form as that used by Cristescu [3] and Cristescu and Bell [4] will be used here

$$\begin{aligned} \sigma &= E_0 \varepsilon && \text{if } \sigma < \sigma_Y \\ \sigma &= \beta(\varepsilon + \varepsilon_0)^{1/\alpha} && \text{if } \sigma > \sigma_Y \ . \end{aligned} \tag{3}$$

In the numerical examples the following values for the constants have been used: $\alpha = 2$; $\beta = 5.6\times10^4$ psi (3937 kgr/cm^2); $E_0 = 10.2\times10^6$ psi (717 000 kgr/cm^2) is the initial Young's modulus; $\sigma_Y = 1100$ psi (77.34 kgr/cm^2) is the yield stress and the corresponding strain is $\varepsilon_Y = 0.00010784$ and $\varepsilon_0 = 0.000278$. By convention σ and ε are positive in compression. The program was written in dimensionless variables so that it can be used for any value of the constants. The stress-strain relation (3) introduces a discontinuity in slope at the yield point, which is, however, of negligible significance for the overall picture of the loading-unloading phenomenon.

During unloading we will assume that Young's modulus decreases with the plastic strain. For simplicity, and in order to see qualitatively the influence of this decrease, a linear decrease of the form

$$E = E_0(1 - Q\,\varepsilon_p) \tag{4}$$

was used. Q is a constant; for Q = 10, E decreases 20 % for $\varepsilon_p = 0.02$. Of course E decreases with ε_p up to a certain value of ε_p only. For very high values of ε_p Young's modulus does not continue to decrease, but rather remains more or less constant (see Jukov [1]). This is the reason why

besides law (4) of variation of E with ε_p another law was considered as well. According to this law, E decreases as ε_p increases only as long as ε_p does not surpass a certain limit ε_p^*. When ε_p surpasses this limit, E does not continue to decrease, but remains constant. Thus, besides (4) in some computed cases the following law is used

$$\begin{aligned} E &= E_o(1 - Q\,\varepsilon_p) \qquad \text{if} \quad \varepsilon_p < \varepsilon_p^* \\ E &= E_o(1 - Q\,\varepsilon_p^*) \qquad \text{if} \quad \varepsilon_p > \varepsilon_p^* \ . \end{aligned} \tag{5}$$

All the equations used in the computer program were developed for E variable as given by (4) or (5). However, the same program can be used for the case $E = E_o$ = constant by making $Q = 0$ everywhere..

By writing (3) in differential form and using (4), the two components of the rate of strain will be obtained from

$$\begin{aligned} \dot{\varepsilon}_e &= \frac{\dot{\sigma}}{E_o(1 - Q\,\varepsilon_p)} \\ \dot{\varepsilon}_p &= \Phi\,\dot{\sigma} \end{aligned} \tag{6}$$

with

$$\Phi = \chi\left[\alpha\left(\frac{E_o}{\beta}\right)^{\alpha}\left(\frac{\sigma}{E_o}\right)^{\alpha-1} - \frac{1}{1 - Q\,\varepsilon_p}\right] \frac{1}{E_o\left[1 - \dfrac{Q\,\dfrac{\sigma}{E_o}}{(1 - Q\varepsilon_p)^2}\right]} \tag{7}$$

and

$$\chi = \begin{cases} 0 & \text{if } \sigma < \sigma_Y \quad \text{or} \quad \sigma_Y < \sigma < \sigma_m(x) \\ 1 & \text{if } \sigma = \sigma_m(x) \ . \end{cases} \tag{8}$$

$\sigma_m(x)$ is the maximum stress reached in the section x of the bar up to the moment under consideration.

If (6)-(8) are added to the relation

$$\varepsilon = \varepsilon_e + \varepsilon_p \tag{9}$$

the form of the constitutive equation which was used in the computation is obtained. The original relations (3) written in integrated form were used only in what is called loading/unloading criteria, i.e. in the computations connected with the checking introduced by (8).

The characteristics of the system (1), (6), and (9) can be written

in the form

$$\frac{dx}{dt} = \pm c \tag{10a}$$

$$dx = 0 \tag{10b}$$

with

$$c = \frac{c_o\sqrt{1 - Q\varepsilon_p}}{\sqrt{1 + E_o\left[1 - Q\varepsilon_p - \frac{\frac{\sigma}{E_o}}{1 - Q\varepsilon_p}Q\right]\Phi}} \tag{11}$$

the velocity of propagation. In (11) $c_o = \sqrt{\frac{E_o}{\rho}}$ is the elastic "bar" velocity in a bar undeformed plastically, ρ is the density (here $\rho = 0.000253$ lb $in^{-4}sec^2$ (0.002757 g $cm^{-4}sec^2$)).

Along (10) the differential relations

$$d\sigma = \mp \rho c\, dv \tag{12a}$$

$$d\varepsilon_p = \Phi\, d\sigma \tag{12b}$$

$$d\varepsilon_e = \left(\frac{1}{E} + \frac{\sigma}{E^2}\frac{dE}{d\varepsilon_p}\frac{\Phi}{E_o}\right)d\sigma \tag{12c}$$

are respectively satisfied (12a) along (10a) and (12b) and (12c) along (10b). In the plastic region (10b) enters twice; in the elastic region (10b) enters once and in all formulas $\Phi = 0$.

By writing the basic equations of the problem as described above, we can pass relatively easily from loading to unloading. All these equations have been rewritten in dimensionless variables. Details of the rather involved numerical method used to find the loading/unloading boundary simultaneously with solutions in the loading and unloading regions are omitted.

3. BOUNDARY AND INITIAL CONDITIONS

The problem to be considered is as follows: A finite-length bar, called "specimen" is initially at rest and undeformed. Anoter bar, identical with the first one, and called "hitter" impacts the specimen longitudinally with a given velocity V. Due to symmetry all the computations have been carried out in the specimen only.

Thus the initial conditions for the specimen are

$$\left.\begin{array}{r} t = 0 \\ 0 < x < \ell \end{array}\right\} \quad \sigma = \varepsilon = v = 0\ . \tag{13}$$

The boundary conditions at the free end are

$$x = \ell, \quad t > 0 \; : \; \sigma = 0 \; , \tag{14}$$

while at the impacted end $x = 0$ three periods can be distinguished

$$0 < t < t^* \; : \; v = v_{max} = \frac{V}{2} \; , \quad \sigma = \sigma_{max} \tag{15a}$$

$$t^* < t < T_c \; : \; v_{specimen} = v_{hitter} \tag{15b}$$

$$T_c < t \; : \; \sigma = 0 \; . \tag{15c}$$

Since the boundary and initial conditions prescribed at $x = 0$, $t = 0$ do not coincide, an elastic shock wave will be formed due to the sudden impact. When reflected from the free end, this elastic shock wave will be an unloading wave traveling back in the bar with the variable velocity

$$c = c_o \sqrt{1 - Q \varepsilon_p} \; . \tag{16}$$

It is gradually absorbed by the direct plastic loading waves. As long as ε_p is small, the equation of the front of this unloading wave is

$$x = - c_o (t - T^*) \tag{17}$$

with $T^* = 2 \ell / c_o$. For greater ε_p, (17) is to be replaced by a curved line whose tangent is

$$dx = - c_o \sqrt{1 - Q \varepsilon_p} \; dt \; . \tag{18}$$

This curve can be plotted only after determining the solution. The curve (18) lies above the straight line (17).

Generally, from the free end up to the point where the reflected elastic shock wave is completely absorbed, $\varepsilon_p < 0.1$ % so that $c \simeq c_o$ and practically (18) does not differ from (17). For the examples given in the present paper, the vertical distance between lines (17) and (18) near the impacted end ranges from 0.18 μsec to 0.5 μsec. For this reason the calculations were actually carried out by using the line (17) in place of the curve (18). This makes it possible to obtain the solution along (17) after the passage of the reflected wave by elementary formulas, and to use further computations, above the line (17), with the computer.

Note that T^* has no special physical meaning (as it would if $E = E_o$) and does not play a significant role in (15), since the condition $v_{specimen} = v_{hitter}$ is satisfied for $t < t^*$ in any case. It is only for a certain time $t > t^*$ which is obtained during computation that v at the end

of the bar becomes smaller than v_{max}. Finally in (15), T_c is the time of contact between the two bars, which is again obtained by computations.

The required unknown functions were computed along the line (17) on both sides of it, as long as this line represents a discontinuity front. The values "before" were obtained from

$$\sigma_b = \frac{\beta^2}{2\varrho c_o^2}\frac{t^2}{(t-t^*)^2}$$

$$v_b = \frac{2}{3\beta}\sqrt{\frac{2}{\varrho}}\,\sigma^{3/2} + \left(\frac{1}{\varrho c_o} - \frac{2}{3\beta}\sqrt{\frac{2}{\varrho}}\sqrt{\sigma_Y}\right)\sigma_Y \qquad (19)$$

$$\varepsilon_b^p = \frac{1 + Q\varepsilon_b - \sqrt{(1+Q\varepsilon_b)^2 - 4Q(\varepsilon_b - \frac{\sigma}{E_o})}}{2Q}$$

$$\varepsilon_b^e = \varepsilon_b - \varepsilon_b^p$$

while the values "after" from the standard jump conditions (see, for instance, Cristescu [2] Ch.II) in which

$$\varepsilon_a^p = \varepsilon_b^p \quad \text{and} \quad \varepsilon_a^e = \frac{\sigma_a}{E_o(1 - Q\varepsilon_a^p)} \qquad (20)$$

With this procedure one obtains the values of all required functions "above" the line (17) and these are used as "initial" data for the computations done with the computer above this line. This procedure has two main advantages. First, one does not use the computer for the solution in the domain below the line (17). Thus, one saves computer time and avoids numerical analysis at the singular point $x = 0$, $t = 0$ and along the discontinuity fronts. Secondly, it is very easy to handle various boundary conditions involving discontinuities.

4. RESULTS

Several examples in which E was assumed to vary with ε_p were computed. The results of these computations were compared with computations in which $E = E_o$ = constant as well as with some available experimental data.

Without giving details concerning the program, the author mentions only that the computations were carried out above line (17) in about 123 000 to 155 000 net points and $\ell = 200\Delta x$. These computations were carried out up to a time surpassing the time of contact by about 35 μsec. By this method

it was possible to obtain the elastic vibration propagating in the nonhomogeneously deformed bar after rebound from the hitter. An IBM 360 Model 65 computer was used to perform the calculations. For each computed case, 4 to 6.8 minutes of computer time were necessary. When E was variable with ε_p the computation time increased about 20% above that for E = constant, because of several additional iterative procedures introduced in the program in both loading and unloading domains.

Two velocities of impact were considered for the boundary conditions: V = 3002 in/sec (76.25 m/sec) and V = 1604 in/sec (40.74 m/sec). To these velocities of impact the following maximum stress correspond, if (3) is used: σ_{max}= 12 750 psi (896.5 kgr/cm^2) and σ_{max}= 8450 psi (594.1 kgr/cm^2). These two cases were considered by Cristescu [3] and Cristescu and Bell [4], respectively, assuming that E is constant. In the latter paper, an extensive comparison between experimental data and theoretical computed results is given. Though reasonably good agreement between experimental and overall behavior of the computed solution was found, there were still discrepancies. Besides the discrepancies near the impacted end which might have been due to the fact that the model used was one-dimensional, there were discrepancies at 3 and 4 diameters from the impacted end (for the magnitude of the maximum strain) and near the free end (for the magnitude of the particle velocity and that of the strain). Thus it was thought that either the model used and/or the loading/unloading mechanism (which was of the classical plasticity theory) should be improved. One purpose of this investigation was to determine whether the reduced unloading elastic modulus might be a significant factor in causing the discrepancies between the experimental data and the calculations made with E = constant.

In the two previously mentioned papers the computations were carried out using a different program from the one used in this paper. Some of the cases presented here with E = constant were recomputed as a check on the new program, and the results obtained were the same.

In order to represent the computed solutions, various graphs were plotted, giving mainly the variations of those functions which can be obtained experimentally as well. All of the experimental data used in this

paper have been obtained by J. F. Bell. Here these were extracted from the paper by Cristescu and Bell [4].

Let us examine first the examples computed for $V = 40.74$ m/sec . Law (4) was used for computing three cases corresponding to $Q = 0$, $Q = 5$, $Q = 10$. Henceforth these cases will be denoted by a number 1-3.

Most significant for the mathematical aspect of the problem are the characteristic planes showing the loading and unloading domains. In Figure 1 the characteristic planes with the loading and unloading domains for the three cases considered are shown, marked L and U, respectively. Point A is the section of the rod where the reflected unloading shock wave is completely absorbed by the direct loading waves. Generally, the U/L boundaries in the various cases considered are distinct mainly in the upper part. Slight differences in the U/L boundaries have a negligible effect on the overall behavior of the solution, and, as Figure 1 shows, only slight differences were found. If E is dependent on ε_p then the loading region becomes narrow and a lengthening (in time) of this region in the characteristic plane takes place. At the same time the upper part of the loading region will more closely approach the free end of the bar. This is due to the decrease of the velocity of propagation of the elastic unloading waves. T_c denotes the time of contact, the time at which the stress at the impacted end drops to zero.

The variation of ε at various sections of the bar is shown in Figure 2. Generally, in the first three diameters from the impacted end the computed solutions are well in agreement with the experimental data. Case 2 gives slightly better agreement than the others at $x = 3D$ (not shown). For 4 and 5 diameters from the impacted end all the solutions depart from the experimental data. At $x = 5D$ the initial rise is fairly well represented by all three cases (slightly better by Case 3). The plateau region of nearly constant strain seems to be represented best by Case 2 after the hump in the experimental data is past. Still further away from the impacted end, at 6.5 and 7 diameters (for which experimental data were available), the computed solutions again depart from the experimental data. However, reasonable agreement can be accepted for the computed Case 3. In order to simplify

Figure 2 only the graphs of variations of ε in time at 8 diameters from the impacted end were given. Case 3 comes closest to the experimental data at the beginning of the curve, but is worst of all in the maximum strain region, where all are greatly different from the experimental values. Note that the discrepancy is even greater than meets the eye, since different strain scales are used for the experimental and calculated curves above the break in the strain axis. The computed maximum strains are almost double the measured strains in the maximum-strain region at $x = 8D$, but the strains at $x = 8D$ are very small in comparison to the strains nearer the impacted end, and these discrepancies have very little effect on the overall deformation. The significant discrepancies at $x = 8D$ may be due to the experimental method used there. The strain records at the earlier sections were obtained by Bell's diffraction grating method, and the plotted curves represent averages for many tests. At $x = 8D$, however, the curve was obtained by an electric resistance strain gauge for only a single test. It was believed that at the very low levels of plastic strain, the electric strain gauge data would be acceptable, but this may not be the case.

Another parameter which can be measured experimentally is the variation of the stress at the impacted end. Though the sudden rise and fall of the stress in what was called the "peak stress" as well as in the "overstress" are not described by the models of the type used here, the overall decrease of the stress during the whole process of unloading should be reasonably well described. The variation of the stress at the impacted end, as obtained in various computed cases is shown in Figure 4. Experimental stress data were not available for the impact velocity of $V = 1604$ in/sec. For a qualitative comparison Figure 4 shows experimental stress measurements at $V = 1436$ in/sec or 38 m/sec. The peak stress, which is present in the experimental data at the beginning of the impact (during the first few microseconds) is not represented in Figure 4. If E is highly dependent on ε_p then the computed time of contact is much higher than the experimental one; however, it is possible, that by assuming E to be variable according to the form (5), or another similar law, a better agreement with the experiment could be obtained as the discussion of Figure 7 will indicate. It is inte-

resting to note that a time of contact equal to or slightly smaller than the experimental one was obtained for $E = E_o$.

In Figure 5 the variations in time of the displacement of various sections of the bar are shown. First the variation in time of the particle velocity was obtained, after which the displacement-time history was obtained by an additional integration. The experimental curves were obtained by integrating velocity-time curves measured by an optical method. Generally for the sections of the bar in the first one-third of the bar, near the impacted end, the agreement between experimental and all theoretical solutions is excellent. For example, in Figure 5 is shown the variation of u at $x = 2$ diameters.

In the median portion of the bar the computed and experimental data are still in reasonably good agreement. However, near the free end, there is an important discrepancy between experimental data and all computed solutions. The computed solutions furnish displacements which are much too low. The highest discrepancy is obtained for the section $x = 10$ diameters, that is, at the free end of the bar, as is shown in Figure 5.

In order to make the present discussion more complete, another example was computed for a much higher velocity of impact of $V = 76.25$ m/sec. No experimental data were available for this case. For this reason the computed solution obtained by assuming E variable with ε_p was compared only with the solution obtained assuming $E = E_o = \text{constant}$. The laws used for the variation of E were of the form (4) with $Q = 5$ and of the form (5) with $Q = 10$ and $\varepsilon_p^* = 0.02$.

The results obtained are somewhat similar to the previous ones. In Figure 6 are shown superposed three characteristic planes showing loading and unloading regions for $E = E_o$ and E variable. The three loading regions obtained for these three cases are different mainly in their upper part. The loading region for E variable is narrower and extended more toward increasing t and toward the free end of the bar. As a result, if E is variable the time of contact is higher and the plastic waves penetrate a little more along the bar than in the case E = constant. This means that although the plastic strains are generally smaller for the case E variable, near the free

end they can be still higher. This can also be seen from Figure 7, which shows the distribution of the plastic strain along the bar for the three computed cases. The biggest difference between the three computed solutions is apparent in the median portion of the bar. It is interesting to observe that with law (4), as Q increases the time of contact increases, but when a law of variation for E of the form (5) is assumed, then the increase in the time of contact is not so great.

All other diagrams showing the variation in time or along the bar of various required functions, are somewhat similar to those obtained for the previous case where V = 40.76 m/sec. These will not be given here.

5. CONCLUSIONS

In the present paper the author has shown what the influence would be of the variation of E with ε_p on the unloading process following the propagation of plastic waves in a bar. Generally, if E is assumed to decrease with ε_p, the whole picture of the unloading process is more or less changed. From the main results that can be checked experimentally we note: if E decreases with ε_p then the time of contact increases, the plastic waves propagate further along the bar, the plastic strain near the impacted end is generally smaller, it is much smaller in the middle of the bar, but bigger near the free end. The conclusion which can be drawn from the previously explained examples must be considered only as indicative pending a careful experimental establishment of the variation of E with ε_p.

If E is dependent on ε_p this implies that measuring the residual plastic strain at various sections after experimentation, and using the usual assumption that E is constant will furnish erroneous information about the maximum stress and strain states from where the unloading elastic behavior has started in that particular section of the bar under consideration.

The possible variations of E with ε_p is only one of several possible aspects which have been thought to improve the description of unloading in dynamic plasticity. The rate-effects have been considered in [5] for exactly the same kind of problem.

ACKNOWLEDGMENTS

The author wishes to express his appreciation to Cornelia Cristescu

for making the program in FORTRAN IV and taking care of the computations. The computations were done at the Computing Center of the University of Florida, for which the author is grateful to the Department of Engineering Science and Mechanics.

REFERENCES

1 JUKOV, A. M. , Elastic Properties of Plastically Deformed Metals and Combined Loading, Inj.Sbornik, tom 30,(1960), 3-16

2 CRISTESCU, N., Dynamic Plasticity, North Holland Pub.Co.,Amsterdam, (1967)

3 CRISTESCU, N., The Unloading in Symmetric Longitudinal Impact of Two Elastic-Plastic Bars, Int.J.Mech.Sci.,Vol. 12, (1970), 723-738

4 CRISTESCU, N. and BELL, J.F., On Unloading in the Symmetrical Impact of Two Aluminum Bars, Proc.Battelle Colloquium, Sept. 1969, McGraw-Hill Book Co., (1970), 397-419

5 CRISTESCU, N., Unloading Solutions in Longitudinal Impact of Bars Exhibiting Both Time-Dependent and Time-Independent Plasticity (to be published).

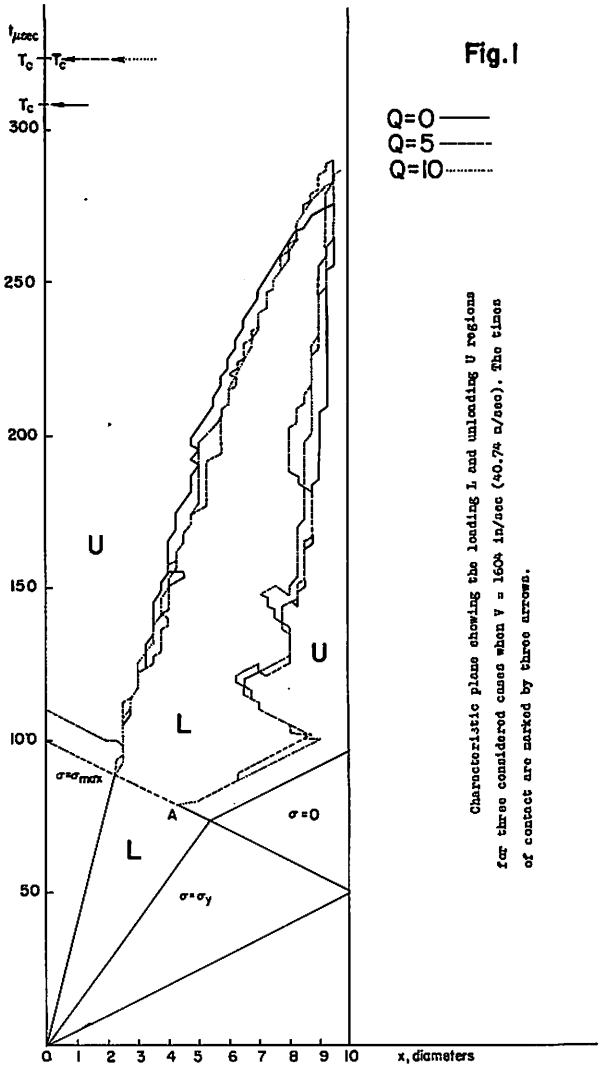

Fig.1

Q=0 ——
Q=5 – – –
Q=10 ·····

Characteristic plane showing the loading L and unloading U regions for three considered cases when V = 1604 in/sec (40.7% c/sec). The times of contact are marked by three arrows.

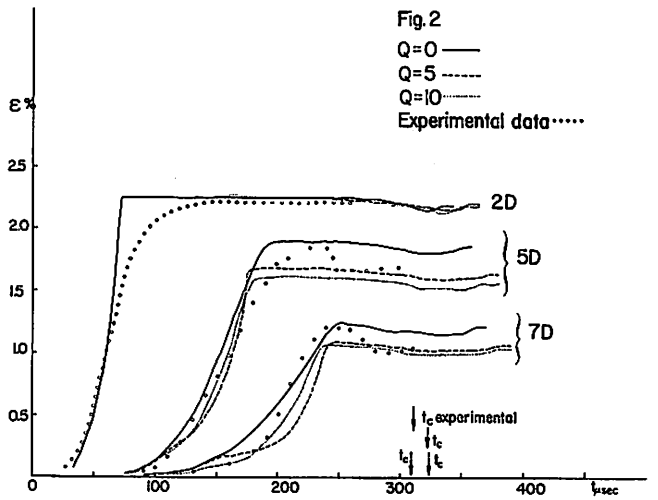

Variation of the strain at various sections of the bar as given by computation and experiment.

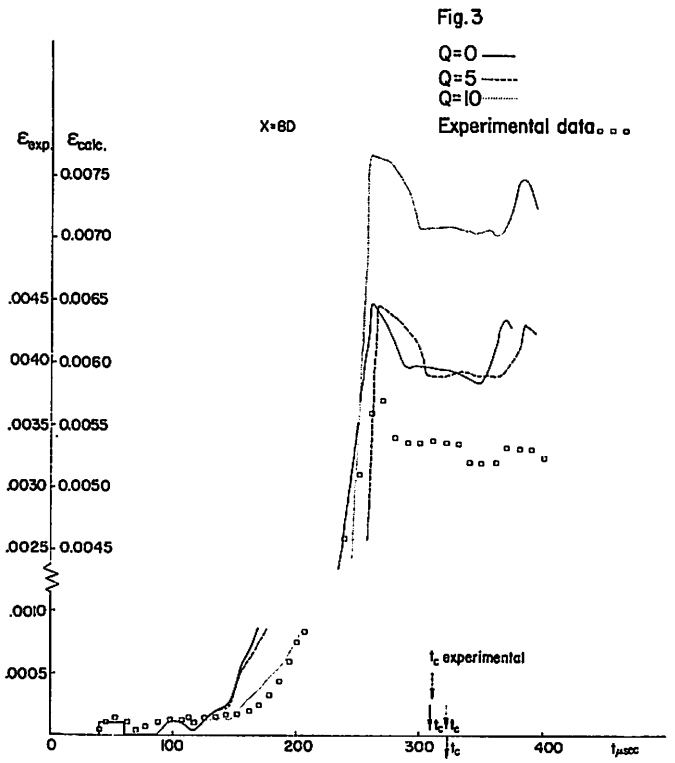

Variation of strain at x = 8D (to note the different scales used for the plotting of the calculated curves and the experimental data).

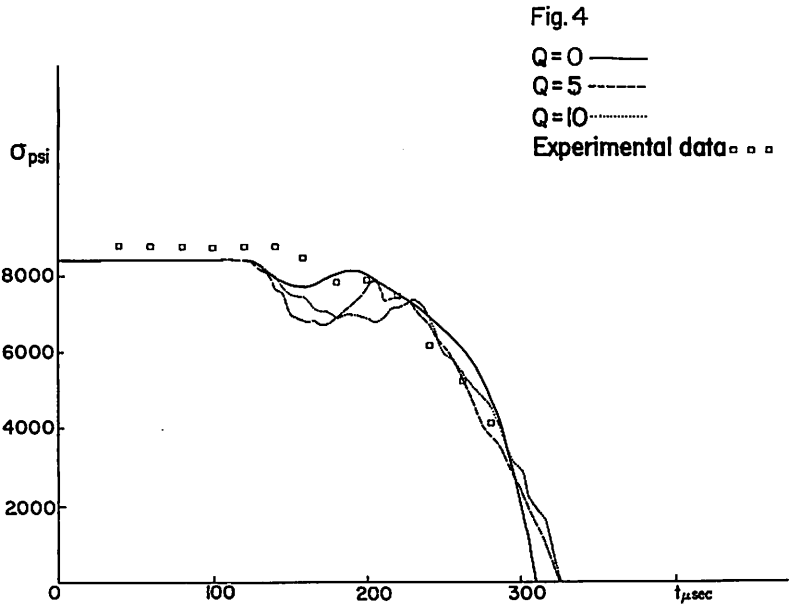

Variation of stress at the impacted end of the bar.

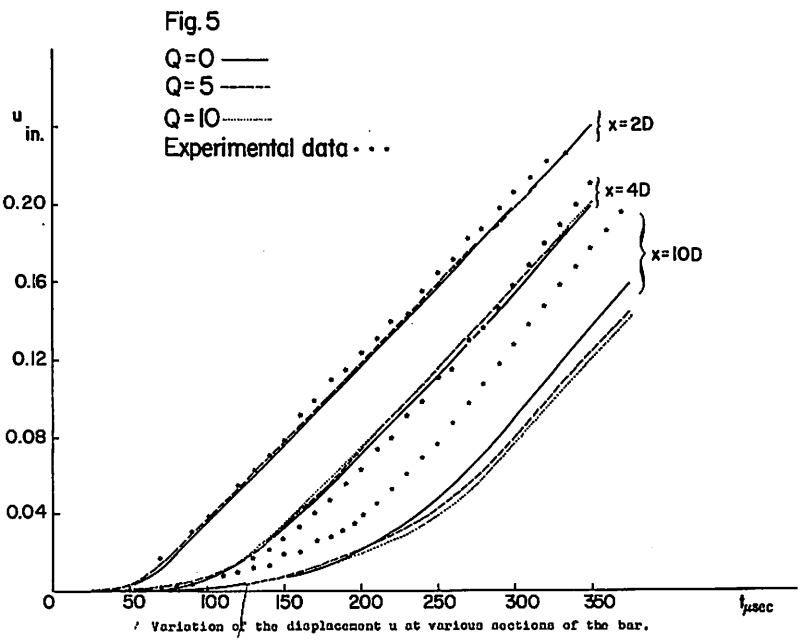

Variation of the displacement u at various sections of the bar.

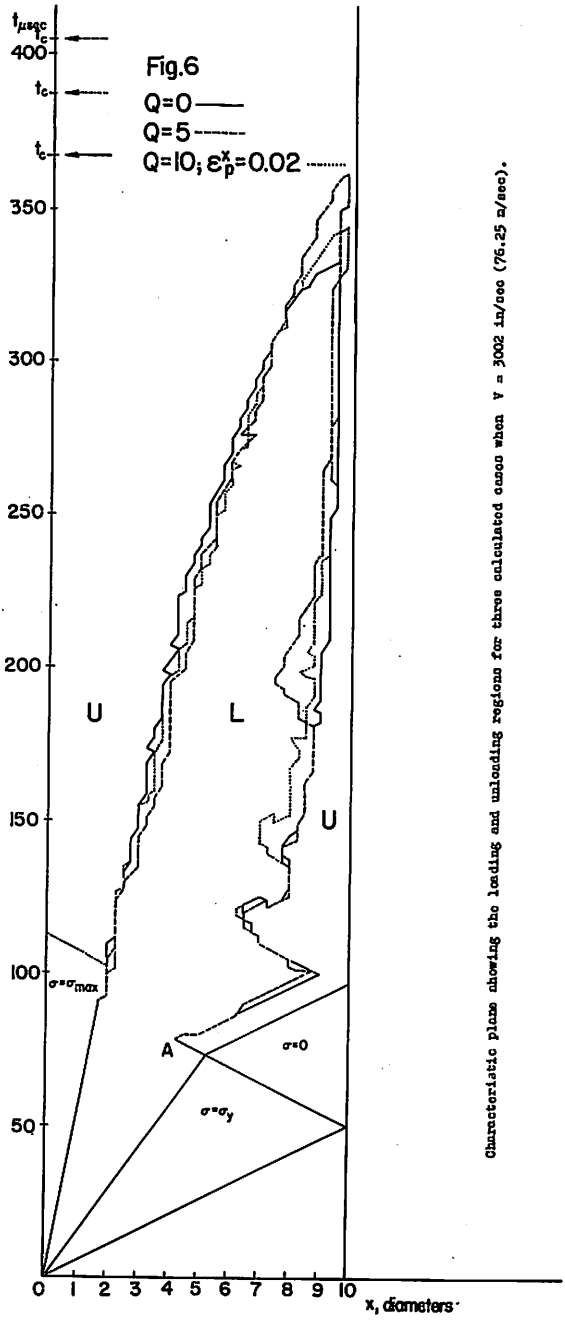

Characteristic plane showing the loading and unloading regions for three calculated cases when V = 3002 in/sec (76.25 m/sec).

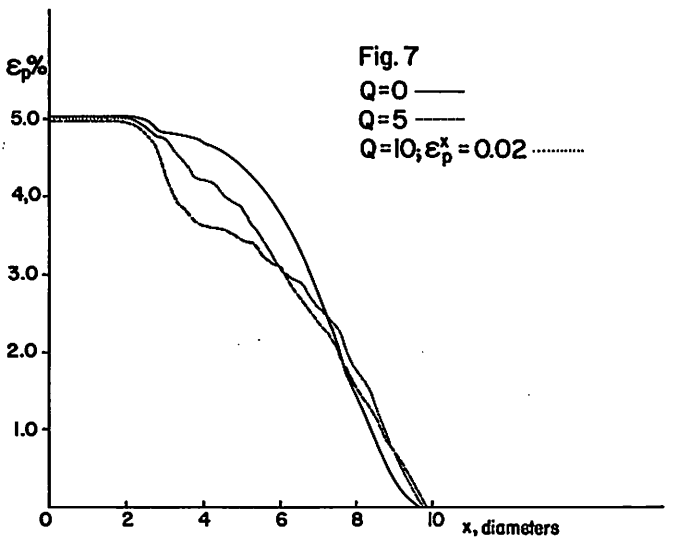

Distribution of plastic strain along the bar as furnished by the computed cases obtained for V = 3002 in/sec (76.25 m/sec).

DISCUSSION

Q A. PHILLIPS, U. S. A.

In one of the slides the curve ε - t seems to indicate strain-rate dependency. Could this be elaborated ?

A N. CRISTESCU, Roumania

Yes, it is true, the changement of curvature of the ε - t curves is a strain-rate effect, as I have shown in one of my papers, now in print.